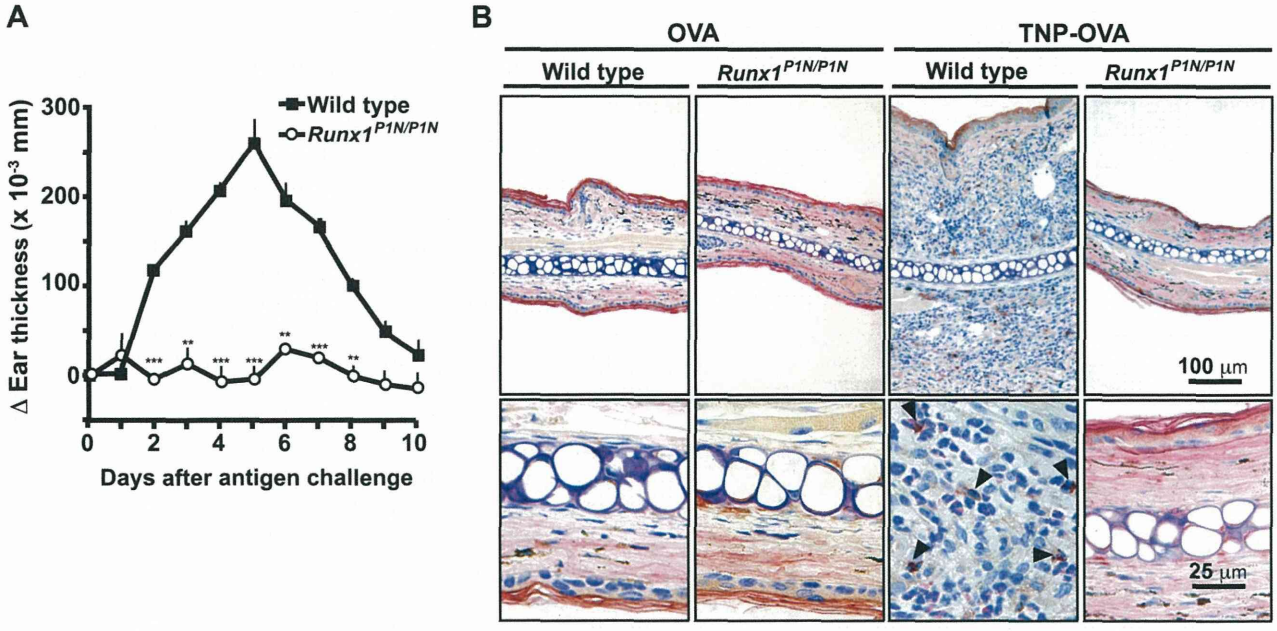

Figure 5. *Runx1*$^{P1N/P1N}$ mice have markedly reduced basophil- and IgE-dependent chronic allergic inflammation. (A) WT (■) or *Runx1*$^{P1N/P1N}$ mice (○) were sensitized passively by an IV injection of TNP-specific IgE 1 day before being challenged with an intradermal injection of TNP-OVA into the left ear pinna and OVA into the right ear pinna as a control. Ear swelling at each time point is shown (means + SEM, n = 3 each). (B) Immunohistochemical staining with an anti-mMCP8 Ab (DAB substrate) to visualize basophils (some indicated with solid arrowheads) and Giemsa counterstaining (4-μm-thick, paraffin-embedded sections) to demonstrate leukocytes in ear pinnae from WT or *Runx1*$^{P1N/P1N}$ mice 4 days after challenge with OVA or TNP-OVA. Scale bars indicate 100 μm (top panel) or 25 μm (bottom panel). Data shown are from 1 of 2 independent experiments, each of which gave similar results. ***$P < .0001$; **$P < .001$; no asterisk, $P > .05$ relative to the corresponding WT mice.

the number of basophils (mIgE$^+$DX5$^+$c-Kit$^-$) in these mice by flow cytometry. In WT mice, we observed an approximately 4-fold increase in BM basophils, and a more than 10-fold increase in spleen basophils (Figure 6A-B). In *Runx1*$^{P1N/P1N}$ mice, basophils exhibited similar increases in response to *S venezuelensis* infection as observed in WT mice, namely, approximately 4.5-fold in the BM and approximately 8-fold in the spleen, but these expanded populations of basophils in *S venezuelensis*–infected *Runx1*$^{P1N/P1N}$ mice were still less than the corresponding basal levels in the uninfected WT mice.

Previous reports from our laboratory and others have shown that IL-3 is essential for the increases in basophil levels that occur after infection with the nematodes *S venezuelensis*[14,15] and *Nippostrongylus brasiliensis*.[15,45] To examine the responsiveness of *Runx1*$^{P1N/P1N}$ mice to IL-3 in vivo, we injected IL-3 (100 ng/d, IP injection for 7 consecutive days) into WT or *Runx1*$^{P1N/P1N}$ mice. IL-3 treatment greatly increased the numbers of basophils in WT mice by approximately 4-fold in both the BM and spleen compared with values in WT mice not treated with IL-3 (Figure 6C-D). As observed with *S venezuelensis* infection, although *Runx1*$^{P1N/P1N}$ mice injected with IL-3 exhibited increases in basophil numbers that were similar or even greater than those of WT mice (approximately 6-fold in the BM and more than 10-fold in the spleen), the numbers of basophils in IL-3–injected *Runx1*$^{P1N/P1N}$ mice remained at levels lower than baseline levels of basophils in vehicle-injected WT mice (Figure 6C-D).

We reported previously evidence that both IL-3 and c-Kit can contribute to resistance to a primary infection with *S venezuelensis*[14] When we examined mast cell– and IL-3–deficient *Kit*$^{W/W\text{-}v}$, IL-3$^{-/-}$ mice, they exhibited a more pronounced defect in rejection of *S venezuelensis* during the primary infection than did either *Kit*$^{W/W\text{-}v}$ or IL-3$^{-/-}$ mice,[14] suggesting that basophils might contribute to host resistance during this infection. *Runx1*$^{P1N/P1N}$ mice cleared a primary infection with *S venezuelensis* significantly more slowly than did WT mice (supplemental Figure 2). Whereas we cannot rule out the possibility that other defects in *Runx1*$^{P1N/P1N}$ mice also contributed to this observation, this finding is consistent with the hypothesis that the impaired response to this infection reflects, at least in part, the drastic reduction in basophils in *Runx1*$^{P1N/P1N}$ mice.

It has been reported that TSLP injection can increase the numbers of basophils in mice.[8] We found that TSLP treatment (400 ng/mouse/d IP for 5 consecutive days) increased the numbers of basophils in the BM and spleen by approximately 50%-100% in both WT mice and *Runx1*$^{P1N/P1N}$ mice (supplemental Figure 3). Moreover, as observed with *S venezuelensis* infection or IL-3 treatment, levels of basophils in TSLP-treated *Runx1*$^{P1N/P1N}$ mice remained lower than baseline levels of basophils in vehicle-treated WT mice.

BaPs are severely reduced in *Runx1*$^{P1N/P1N}$ mice

To examine whether the reduced numbers of basophils in *Runx1*$^{P1N/P1N}$ mice are associated with a deficit in BaPs, we first performed flow cytometric analysis of granulocyte progenitors in the BM. We showed previously that SN-Flk2$^+$ (Sca-1$^-$Lin$^-$ c-Kit$^+$CD150$^-$ Flk2$^+$CD27$^+$) and SN-Flk2$^-$ (Sca-1$^-$Lin$^-$ c-Kit$^+$CD150$^-$Flk2$^-$CD27$^+$) populations are already committed predominantly to the granulocyte fate, and that these populations can give rise to all 3 kinds of granulocytes.[35] There were no significant differences between WT and *Runx1*$^{P1N/P1N}$ mice in SN-Flk2$^+$ or SN-Flk2$^-$ (Figure 7A).

We next assessed BaPs (Lin$^-$CD34$^+$c-Kit$^-$FcεRIα$^+$), which have been shown to differentiate predominantly into basophils.[12] BaPs were severely reduced in *Runx1*$^{P1N/P1N}$ mice (Figure 7B). Ohmori et al reported that treatment with a mixture of IL-3 and anti–IL-3 (the IL-3 complex) increased the frequency of BaPs in WT mice.[13] Compared with IL-3 treatment, injection of the IL-3 complex resulted in a more substantial increase in basophils

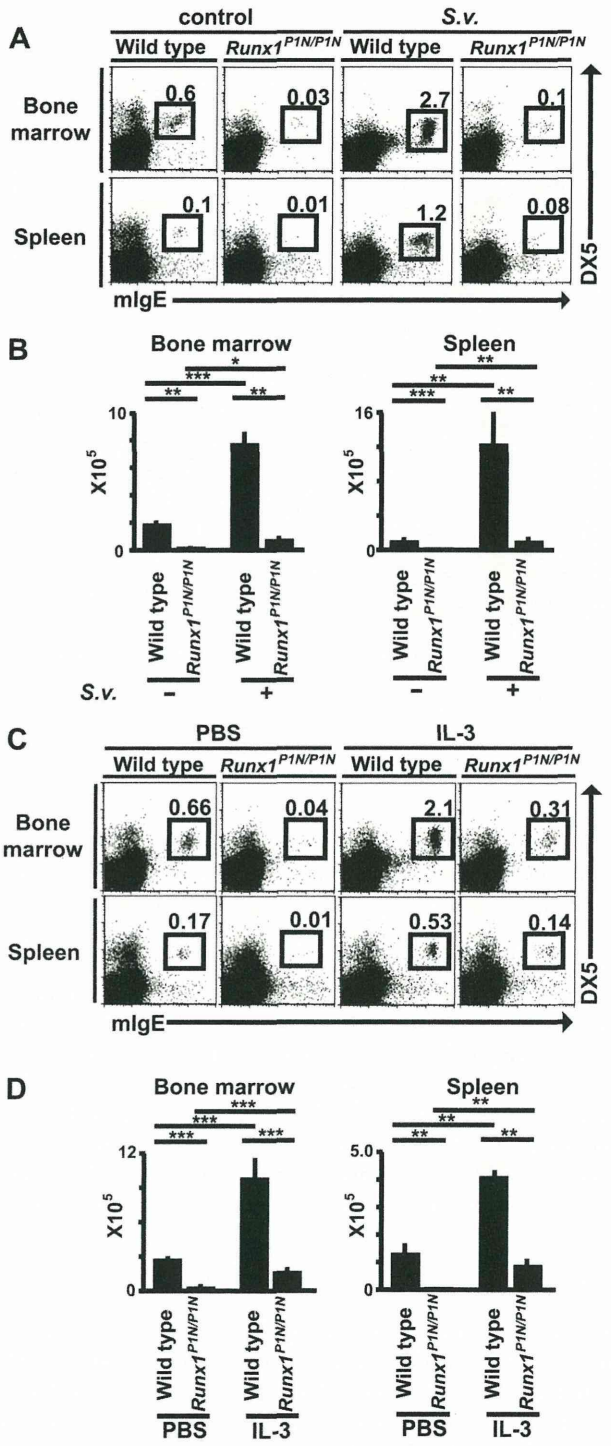

Figure 6. Changes in basophil numbers after *S venezuelensis* infection or IL-3 injection in *Runx1*$^{P1N/P1N}$ versus WT mice. (A) WT or *Runx1*$^{P1N/P1N}$ mice were infected with 10 000 *S venezuelensis* larvae and basophils (mIgE$^+$DX5$^+$) in the BM and spleen were analyzed 8 days after infection. Data shown are from 1 of 3 independent experiments, each of which gave similar results. (B) Recombinant IL-3 (200 ng/mouse/d) was injected into WT or *Runx1*$^{P1N/P1N}$ mice for 7 consecutive days. Basophils in the BM and spleen from each mouse were stained the day after the 7th injection. Data shown in panels B and D are means + SEM.

(supplemental Figure 4A-B). IL-3 complex treatment also resulted in an increase of BM BaPs. As shown in supplemental Figure 4A and B, treatment with the IL-3 complex resulted in substantial increases of BaPs in both WT mice and *Runx1*$^{P1N/P1N}$ mice. As was also observed for basophils, injection of IL-3 complex into *Runx1*$^{P1N/P1N}$ mice resulted in levels of BaPs that were higher than the baseline levels of these cells in WT mice, but that were still much less than the corresponding levels of these cells in IL-3 complex–treated WT mice.

Akashi et al reported the identification of a Lin$^-$c-Kit$^+$β7$^+$FcγRII/III$^+$ BMCP in the spleen.[12] However, we detected no difference in the numbers of Lin$^-$c-Kit$^+$β7$^+$FcγRII/III$^+$ cells in the spleens of WT compared with *Runx1*$^{P1N/P1N}$ mice (Figure 7C).

To examine their developmental potential, we performed single-cell cultures of SN-Flk2$^+$ and SN-Flk2$^-$ cells. We sorted each of these progenitors to a single cell per well and, after 7 and 11 days of culture, analyzed the resulting populations by assessing their surface markers by flow cytometry and their morphology by cytospin analysis. In the case of BaPs, we sorted 100 cells per well from WT mice (we could not collect enough to analyze from *Runx1*$^{P1N/P1N}$ mice), and analyzed them 7 days after culture. Neutrophils were defined as Gr-1^{high} cells with lobulated nuclei and no Vital Red staining of the cytoplasm, eosinophils as Gr-1^{int} CCR3$^+$ cells with lobulated nuclei that exhibited cytoplasmic staining with Vital Red, basophils as Gr-1$^-$FcεRI$^+$c-Kit$^-$DX5$^+$ cells with lobulated nuclei and with cytoplasm that stained with mMCP-8 but not with Vital Red, and mast cells as Gr-1$^-$FcεRI$^+$ c-Kit$^+$DX5$^-$ cells lacking Vital Red and mMCP-8 staining of the cytoplasm (supplemental Figure 5).

As shown in supplemental Figure 6, neutrophils developed from both SN-Flk2$^+$ and SN-Flk2$^-$ cells and there were no differences between results obtained from cells derived from WT versus *Runx1*$^{P1N/P1N}$ mice. Compared with neutrophils, eosinophils developed more efficiently from SN-Flk2$^-$ than SN-Flk2$^+$ cells, but there were also no significant differences between results obtained from cells derived from WT versus *Runx1*$^{P1N/P1N}$ mice. Basophils developed predominantly from SN-Flk2$^-$ cells in WT mice, but that potential was severely reduced in SN-Flk2$^-$ cells from *Runx1*$^{P1N/P1N}$ mice. As expected, BaPs from WT mice developed into basophils (supplemental Figure 6). In contrast, Lin$^-$c-Kit$^+$β7$^+$FcγRII/III$^+$ "BMCPs" gave rise only to mast cells whether we used our culture conditions ("5 cytokines" in supplemental Figure 7) or those used by Akashi et al[12] ("10 cytokines" in supplemental Figure 7).

Together with our finding of a striking reduction in basophils in *Runx1*$^{P1N/P1N}$ mice in vivo, these in vitro results indicate that P1-Runx1 plays a role in facilitating the developmental transition from granulocyte progenitors to BaPs, and that an abnormality at this step contributes to the drastic reduction in basophils in *Runx1*$^{P1N/P1N}$ mice. Our data also suggest that Lin$^-$ c-Kit$^+$β7$^+$FcγRII/III$^+$ cells do not represent the main pathway for the development of basophils in vivo.

Discussion

In the present study, we found that *Runx1*$^{P1N/P1N}$ mice, which are deficient in the P1-Runx1 transcription factor, exhibit a severe reduction in basophils at baseline (Figure 1), but have normal levels of other granulocytes and tissue mast cells (Figure 3). To our knowledge, our data are the first to identify P1-Runx1 as a transcription factor that has a nonredundant role in the development of basophils but apparently not for other granulocytes or mast cells. We reported previously that granulocyte development potential resides predominantly in SN-Flk2$^+$ (Sca-1$^-$Lin$^-$ c-Kit$^+$CD150$^-$Flk2$^+$ CD27$^+$) and SN-Flk2$^-$ (Sca-1$^-$Lin$^-$c-Kit$^+$ CD150$^-$Flk2$^-$CD27$^+$) populations.[35] In the present study, we

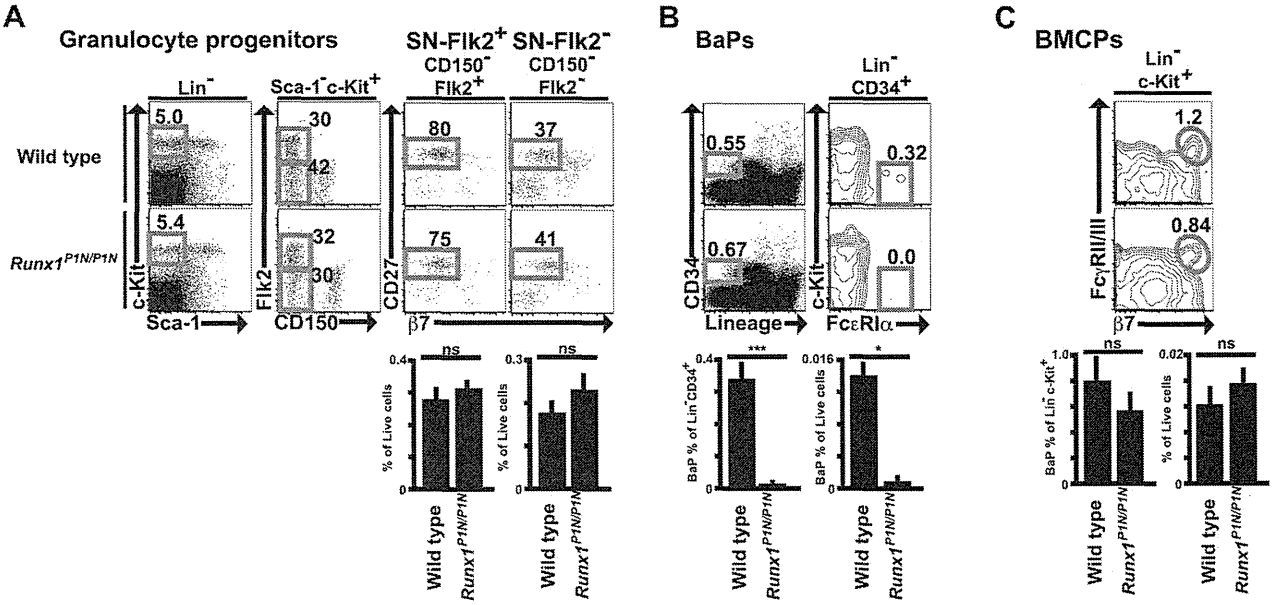

Figure 7. Impaired BaPs in *Runx1*$^{P1N/P1N}$ mice. (A-C) Representative flow cytometry plots and percentage of indicated gates of SN-Flk2$^+$ (Sca-1$^-$Lin$^-$c-Kit$^+$CD150$^-$Flk2$^+$CD27$^+$) cells and SN-Flk2$^-$ (Sca-1$^-$Lin$^-$c-Kit$^+$CD150$^-$Flk2$^-$ CD27$^+$) cells (A), and BaPs (Lin$^-$CD34$^+$c-Kit$^-$FcεRIα$^+$) in BM from WT or *Runx1*$^{P1N/P1N}$ mice (B), and BMCPs (Lin$^-$c-Kit$^+$β7$^+$FcγRII/III$^+$) in spleen from WT or *Runx1*$^{P1N/P1N}$ mice (C). Data shown are from 1 of 3 independent experiments, each of which gave similar results.

found that the SN-Flk2$^+$ and SN-Flk2$^-$ populations are present in normal numbers in *Runx1*$^{P1N/P1N}$ mice (Figure 7A), but that the number of BaPs[12] is reduced profoundly in such mice (Figure 7B). These findings suggest that *Runx1*$^{P1N/P1N}$ mice have a marked restriction in the transition from granulocyte progenitors to BaPs.

It is important to emphasize that whereas basophils levels are strikingly reduced in *Runx1*$^{P1N/P1N}$ mice, a few basophils can be still detected in these mice (Figure 1). Moreover, when we subjected *Runx1*$^{P1N/P1N}$ mice either to infection with the nematode *S venezuelensis* or to repetitive injection with IL-3, each of which results in marked expansion of basophil populations in WT mice,[13-15] basophil numbers also expanded in *Runx1*$^{P1N/P1N}$ mice (Figure 6). Indeed, although basophil numbers in *S venezuelensis*–infected or IL-3–injected *Runx1*$^{P1N/P1N}$ mice remained lower than the corresponding baseline levels in naive WT mice, the relative increases in the numbers of BM and spleen basophils in *S venezuelensis*–infected or IL-3–injected *Runx1*$^{P1N/P1N}$ mice were the same as or greater than those in the identically treated WT mice (Figure 6). These findings indicate that the basophil lineage in *Runx1*$^{P1N/P1N}$ mice retains responsiveness to IL-3, but that the expansion of basophils in *Runx1*$^{P1N/P1N}$ mice injected with IL-3 or infected with a parasite that results in enhanced levels of endogenous IL-3 is subject to a marked restriction, as is the development of baseline levels of basophils in these mice.

In addition to the apparently unipotential BaPs, Arinobu et al reported that a Lin$^-$c-Kit$^+$β7$^+$FcγRII/III$^+$ bipotent progenitor of basophils and mast cells (which they named "BMCP") can be identified by flow cytometry in the mouse spleen.[12] We found that *Runx1*$^{P1N/P1N}$ and WT mice have similar numbers of Lin$^-$c-Kit$^+$β7$^+$FcγRII/III$^+$ cells in the spleen (Figure 7C). However, in the present study, these cells gave rise only to mast cells in vitro. In analyzing the cultured cells, we identified basophils by both flow cytometry (as FcεRIα$^+$DX5$^+$c-Kit$^-$ cells) and by morphology (as cells with lobulated and often ring-like nuclei and exhibiting a few granules in the cytoplasm by Giemsa stain and positive staining of the cytoplasm with an Ab to mMCP-8). Mast cells were defined as FcεRIα$^+$DX5$^-$c-Kit$^+$ cells by flow cytometry and by morphology as mMCP-8$^-$ cells with many granules in the cytoplasm that stained with Giemsa stain.

It is possible that the discrepancy between our findings and those of Arinobu et al[12] reflect differences in the mice analyzed and/or in aspects of the flow cytometric or culture conditions used. However, we found using flow cytometry that *Runx1*$^{P1N/P1N}$ mice and WT mice not only have similar numbers of Lin$^-$c-Kit$^+$β7$^+$FcγRII/III$^+$ "BMCPs" in the spleen (Figure 6C), but also exhibit statistically indistinguishable numbers of mast cells in the peripheral tissues analyzed (Figure 3). Our data thus indicate that Lin$^-$c-Kit$^+$β7$^+$FcγRII/III$^+$ cells may have only a limited (or no) ability to give rise to basophils. As we suggested in a prior study,[35] Lin$^-$c-Kit$^+$β7$^+$FcγRII/III$^+$ cells may represent mast-cell progenitors that can give rise to a subpopulation of cells in the mast-cell lineage that have little or no surface expression of c-Kit.[46] Moreover, mouse basophils can be difficult to identify based on conventional staining protocols (such as with May-Giemsa staining). We therefore recommend confirming the identity of mouse basophil populations initially identified based on testing a limited number of cell-surface markers by also searching for markers that are more specific for these cells, such as mMCP-8.

The precise mechanism by which P1-Runx1 regulates basophil differentiation remains to be elucidated. One must consider in this context at least 2 pathways of basophil development. The first is basophil differentiation in naive mice at baseline. In this pathway, both IL-3 and TSLP are dispensable.[8,14,15] Alternatively, during infection with certain parasites, IL-3 is essential for basophil expansion,[14,15,45] and it has been reported that injections of the IL-3 complex can result in an increase in the number of BaPs and basophils.[13] We detected no significant differences in the levels of surface expression of the IL-3 receptor on basophils or SN-Flk progenitors in WT compared with *Runx1*$^{P1N/P1N}$ mice (data not shown). Moreover, whereas treatment with the IL-3 complex is not "physiologic," such experiments revealed that IL-3 can increase numbers of both basophils and BaPs in *Runx1*$^{P1N/P1N}$ mice and in WT mice (supplemental Figure 4). These results provide further

support for the conclusion that the defect(s) in basophil production in *Runx1*$^{P1N/P1N}$ mice occur despite the retention of responsiveness of cells in the basophil lineage to IL-3 and TSLP.

Based on these results, we speculate that the P1-Runx1 pathway functions in parallel with or independently of the IL-3 or TSLP-dependent pathways. Indeed, because we observed a substantial increase in basophil numbers over baseline levels in *S venezuelensis*–infected or IL-3–treated *Runx1*$^{P1N/P1N}$ mice (Figure 6), and because basophils were not completely absent in *Runx1*$^{P1N/P1N}$ mice in the steady state (although basophil numbers were < 10% of WT levels; Figure 1), there appears to be a P1-Runx1–independent pathway that can contribute to the development of basophils both at baseline and during IL-3–dependent (and perhaps TSLP-dependent) expansion of this cell type. It is possible that IL-3 and TSLP are not the only contributors that regulate basophil numbers and that P1-Runx1 can modulate the action of those other regulators/mechanisms of basophil development. Clearly, further studies are required to clarify the identity and interrelationships among the pathways that contribute to basophil development.

The results of the present study reveal a novel role for P1-Runx1 in basophil development and provide another example of a difference in the regulation of basophil and mast-cell development in mice. Our findings also suggest that further studies of P1-Runx1–mediated transcriptional networks may uncover additional interesting features of the developmental pathway(s) that lead(s) to the generation of these rare and enigmatic granulocytes.

Acknowledgments

The authors thank Chieko Tezuka, Chen Liu, and Jennifer Lilla for technical assistance; Fu-Tong Liu for providing ε-26 IgE; and all the members of the Galli, Karasuyama, and Taniuchi laboratories for helpful discussions.

This study was supported by grants from the National Institutes of Health (AI070813, AI023990, and CA072074 to S.J.G.) and the Japanese Ministry of Education, Culture, Sports, Science and Technology (to I.T. and K.N.).

Authorship

Contribution: K.M., M.J.B., M.T., and K.N. performed the experiments; K.M., M.J.B., M.T., K.N., H.K., I.T., and S.J.G. designed the research and analyzed the data; K.M. and S.J.G. wrote the manuscript; and all authors reviewed and edited the manuscript.

Conflict-of-interest disclosure: The authors declare no competing financial interests.

Correspondence: Stephen J. Galli, MD, Department of Pathology, L-235, Stanford University School of Medicine, 300 Pasteur Dr, Stanford, CA 94305-5324; e-mail: sgalli@stanford.edu.

References

1. Galli SJ. Mast cells and basophils. *Curr Opin Hematol.* 2000;7(1):32-39.
2. Gibbs BF. Human basophils as effectors and immunomodulators of allergic inflammation and innate immunity. *Clin Exp Med.* 2005;5(2):43-49.
3. Sullivan BM, Locksley RM. Basophils: a nonredundant contributor to host immunity. *Immunity.* 2009;30(1):12-20.
4. Nakanishi K. Basophils as APC in Th2 response in allergic inflammation and parasite infection. *Curr Opin Immunol.* 2010;22(6):814-820.
5. Sokol CL, Medzhitov R. Role of basophils in the initiation of Th2 responses. *Curr Opin Immunol.* 2010;22(1):73-77.
6. Karasuyama H, Mukai K, Obata K, Tsujimura Y, Wada T. Nonredundant roles of basophils in immunity. *Annu Rev Immunol.* 2011;29:45-69.
7. Schroeder JT. Basophils: emerging roles in the pathogenesis of allergic disease. *Immunol Rev.* 2011;242(1):144-160.
8. Siracusa MC, Saenz SA, Hill DA, et al. TSLP promotes interleukin-3-independent basophil haematopoiesis and type 2 inflammation. *Nature.* 2011;477(7363):229-233.
9. Voehringer D. Basophils in immune responses against helminths. *Microbes Infect.* 2011;13(11):881-887.
10. Voehringer D. Basophils in allergic immune responses. *Curr Opin Immunol.* 2011;23(6):789-793.
11. Min B, Brown MA, Legros G. Understanding the roles of basophils: breaking dawn. *Immunology.* 2012;135(3):192-197.
12. Arinobu Y, Iwasaki H, Gurish MF, et al. Developmental checkpoints of the basophil/mast cell lineages in adult murine hematopoiesis. *Proc Natl Acad Sci U S A.* 2005;102(50):18105-18110.
13. Ohmori K, Luo Y, Jia Y, et al. IL-3 induces basophil expansion in vivo by directing granulocyte-monocyte progenitors to differentiate into basophil lineage-restricted progenitors in the bone marrow and by increasing the number of basophil/mast cell progenitors in the spleen. *J Immunol.* 2009;182(5):2835-2841.
14. Lantz CS, Boesiger J, Song CH, et al. Role for interleukin-3 in mast-cell and basophil development and in immunity to parasites. *Nature.* 1998;392(6671):90-93.
15. Lantz CS, Min B, Tsai M, Chatterjea D, Dranoff G, Galli SJ. IL-3 is required for increases in blood basophils in nematode infection in mice and can enhance IgE-dependent IL-4 production by basophils in vitro. *Lab Invest.* 2008;88(11):1134-1142.
16. Wang ND, Finegold MJ, Bradley A, et al. Impaired energy homeostasis in C/EBP alpha knockout mice. *Science.* 1995;269(5227):1108-1112.
17. Cui Y, Riedlinger G, Miyoshi K, et al. Inactivation of Stat5 in mouse mammary epithelium during pregnancy reveals distinct functions in cell proliferation, survival, and differentiation. *Mol Cell Biol.* 2004;24(18):8037-8047.
18. Collins A, Littman DR, Taniuchi I. RUNX proteins in transcription factor networks that regulate T-cell lineage choice. *Nat Rev Immunol.* 2009;9(2):106-115.
19. Okuda T, van Deursen J, Hiebert SW, Grosveld G, Downing JR. AML1, the target of multiple chromosomal translocations in human leukemia, is essential for normal fetal liver hematopoiesis. *Cell.* 1996;84(2):321-330.
20. Ito Y. RUNX genes in development and cancer: regulation of viral gene expression and the discovery of RUNX family genes. *Adv Cancer Res.* 2008;99:33-76.
21. Ducy P, Zhang R, Geoffroy V, Ridall AL, Karsenty G. Osf2/Cbfa1: a transcriptional activator of osteoblast differentiation. *Cell.* 1997;89(5):747-754.
22. Komori T, Yagi H, Nomura S, et al. Targeted disruption of Cbfa1 results in a complete lack of bone formation owing to maturational arrest of osteoblasts. *Cell.* 1997;89(5):755-764.
23. Inoue K, Ozaki S, Shiga T, et al. Runx3 controls the axonal projection of proprioceptive dorsal root ganglion neurons. *Nat Neurosci.* 2002;5(10):946-954.
24. Levanon D, Brenner O, Otto F, Groner Y. Runx3 knockouts and stomach cancer. *EMBO Rep.* 2003;4(6):560-564.
25. Li QL, Ito K, Sakakura C, et al. Causal relationship between the loss of RUNX3 expression and gastric cancer. *Cell.* 2002;109(1):113-124.
26. Wang Q, Stacy T, Miller JD, et al. The CBFbeta subunit is essential for CBFalpha2 (AML1) function in vivo. *Cell.* 1996;87(4):697-708.
27. Taniuchi I, Osato M, Egawa T, et al. Differential requirements for Runx proteins in CD4 repression and epigenetic silencing during T lymphocyte development. *Cell.* 2002;111(5):621-633.
28. Egawa T, Eberl G, Taniuchi I, et al. Genetic evidence supporting selection of the Valpha14i NKT cell lineage from double-positive thymocyte precursors. *Immunity.* 2005;22(6):705-716.
29. Egawa T, Tillman RE, Naoe Y, Taniuchi I, Littman DR. The role of the Runx transcription factors in thymocyte differentiation and in homeostasis of naive T cells. *J Exp Med.* 2007;204(8):1945-1957.
30. Setoguchi R, Tachibana M, Naoe Y, et al. Repression of the transcription factor Th-POK by Runx complexes in cytotoxic T cell development. *Science.* 2008;319(5864):822-825.
31. Ichikawa M, Asai T, Saito T, et al. AML-1 is required for megakaryocytic maturation and lymphocytic differentiation, but not for maintenance of hematopoietic stem cells in adult hematopoiesis. *Nat Med.* 2004;10(3):299-304.
32. Levanon D, Groner Y. Structure and regulated expression of mammalian RUNX genes. *Oncogene.* 2004;23(24):4211-4219.
33. Bee T, Liddiard K, Swiers G, et al. Alternative Runx1 promoter usage in mouse developmental hematopoiesis. *Blood Cells Mol Dis.* 2009;43(1):35-42.
34. Bee T, Swiers G, Muroi S, et al. Nonredundant roles for Runx1 alternative promoters reflect their activity at discrete stages of developmental hematopoiesis. *Blood.* 2010;115(15):3042-3050.
35. Franco CB, Chen CC, Drukker M, Weissman IL, Galli SJ. Distinguishing mast cell and granulocyte

differentiation at the single-cell level. *Cell Stem Cell.* 2010;6(4):361-368.

36. Ugajin T, Kojima T, Mukai K, et al. Basophils preferentially express mouse Mast Cell Protease 11 among the mast cell tryptase family in contrast to mast cells. *J Leukoc Biol.* 2009;86(6):1417-1425.
37. Mukai K, Matsuoka K, Taya C, et al. Basophils play a critical role in the development of IgE-mediated chronic allergic inflammation independently of T cells and mast cells. *Immunity.* 2005; 23(2):191-202.
38. Rudolph AK, Burrows PD, Wabl MR. Thirteen hybridomas secreting hapten-specific immunoglobulin E from mice with Iga or Igb heavy chain haplotype. *Eur J Immunol.* 1981;11(6):527-529.
39. Liu FT, Bohn JW, Ferry EL, et al. Monoclonal dinitrophenyl-specific murine IgE antibody: preparation, isolation, and characterization. *J Immunol.* 1980;124(6):2728-2737.
40. Tachibana M, Tenno M, Tezuka C, Sugiyama M, Yoshida H, Taniuchi I. Runx1/Cbfbeta2 complexes are required for lymphoid tissue inducer cell differentiation at two developmental stages. *J Immunol.* 2011;186(3):1450-1457.
41. Stone KD, Prussin C, Metcalfe DD. IgE, mast cells, basophils, and eosinophils. *J Allergy Clin Immunol.* 2010;125(2 Suppl 2):S73-80.
42. Wershil BK, Mekori YA, Murakami T, Galli SJ. 125I-fibrin deposition in IgE-dependent immediate hypersensitivity reactions in mouse skin. Demonstration of the role of mast cells using genetically mast cell-deficient mice locally reconstituted with cultured mast cells. *J Immunol.* 1987; 139(8):2605-2614.
43. Obata K, Mukai K, Tsujimura Y, et al. Basophils are essential initiators of a novel type of chronic allergic inflammation. *Blood.* 2007;110(3):913-920.
44. Voehringer D, Shinkai K, Locksley RM. Type 2 immunity reflects orchestrated recruitment of cells committed to IL-4 production. *Immunity.* 2004;20(3):267-277.
45. Shen T, Kim S, Do JS, et al. T cell-derived IL-3 plays key role in parasite infection-induced basophil production but is dispensable for in vivo basophil survival. *Int Immunol.* 2008;20(9):1201-1209.
46. Baroni E, Biffi M, Benigni F, et al. VDR-dependent regulation of mast cell maturation mediated by 1,25-dihydroxyvitamin D3. *J Leukoc Biol.* 2007; 81(1):250-262.

Artemin causes hypersensitivity to warm sensation, mimicking warmth-provoked pruritus in atopic dermatitis

Hiroyuki Murota, MD, PhD,[a] Mayuko Izumi, MSc,[a] Mostafa I. A. Abd El-Latif, MD, PhD,[a,b] Megumi Nishioka, MD,[a] Mika Terao, MD, PhD,[a] Mamori Tani, MD,[a] Saki Matsui, MD,[a] Shigetoshi Sano, MD, PhD,[c] and Ichiro Katayama, MD, PhD[a] *Osaka and Kochi, Japan, and Cairo, Egypt*

Background: Itch impairs the quality of life for many patients with dermatoses, especially atopic dermatitis (AD), and is frequently induced by a warm environment.
Objective: To determine the mechanism underlying itch induction by warmth, we focused on artemin, a member of glial cell line–derived neurotrophic factors (GDNFs).
Methods: A gene array assay revealed that artemin was expressed in substance P–treated dermal fibroblasts. The expression of artemin in healthy and AD-lesional skin was evaluated with immunohistochemistry and *in situ* hybridization. The impact of fibroblast-derived artemin on the proliferation and morphology of neural cell was investigated *in vitro*. To confirm the involvement of artemin in skin sensibility, wild-type and GDNF family receptor α3 knockout mice were employed for sensory examination.
Results: Artemin-expressing fibroblasts accumulated in skin lesions of patients with AD. Artemin induced cell proliferation of a neuroblastoma cell line *in vitro*, and intradermal injection of artemin in mice resulted in peripheral nerve sprouting and thermal hyperalgesia. Artemin-treated mice demonstrated scratching behavior in a warm environment, but mice deficient for GDNF family receptor α3, a potent artemin receptor, did not show this behavior. Furthermore, the escaping response to heat stimulus was attenuated in GDNF family receptor α3 knockout mice, suggesting that artemin may contribute to sensitivity to heat.
Conclusion: These data suggest that dermal fibroblasts secrete artemin in response to substance P, leading to abnormal peripheral innervation and thermal hyperalgesia. We hypothesize that artemin lowers the threshold of temperature-dependent itch sensation and might therefore be a novel therapeutic target for treating pruritic skin disorders, including AD. (J Allergy Clin Immunol 2012;130:671-82.)

Key words: Artemin, fibroblast, substance P, atopic dermatitis, itch, nerve fiber, warmth

Itch is the major symptom of inflammatory skin diseases and impairs the quality of life of patients.[1-3] Because itch-induced scratching behavior worsens skin conditions and leads to a vicious itch-scratching cycle,[2,4,5] antipruritic treatment plays a central role in these diseases.[6] An accurate understanding of the mechanisms that cause itch in various skin disorders will contribute to formulate therapies. Several factors are reported to exacerbate itch clinically, and heat-/warmth-provoked itching, in particular, occurs with high frequency.[4,7] Although excessive response to warmth or light mechanical stimuli has been thought of as alloknesis caused by central/peripheral processing sensitization,[4,7] the relationship between heat sensation and itch is less well understood. In previous reports, pruritogens such as histamine and substance P (SP) are described as mediators of alloknesis.[8-10] These factors will contribute to cause alloknesis via affecting various types of cells.[11] However, specific factors that induce warmth-evoked itch remain obscure. In the face of this concern, we focused on the fact that cutaneous nerve fibers are ordinarily localized in dermis and made a hypothesis that dermal fibroblast-derived factors might affect cutaneous nerve fibers and cause alloknesis to warm sensation. To investigate this hypothesis, expression profiling was performed to identify genes induced by histamine or SP treatment in fibroblasts. The results led us to focus on *de novo* artemin gene transcription in fibroblasts after SP stimulation.

Artemin is a member of the glial cell line–derived neurotrophic factor (GDNF)-related family, which includes GDNF, neurturin, and persephin.[12-15] Members of this family are thought to act through a multireceptor complex composed of GDNF family receptor α (GFRα) and the receptor tyrosine kinase product of the c-ret proto-oncogene.[16,17] Four distinct GFRαs (GFRα1-4) have been described in the literature as preferentially binding to GDNF family proteins.[18] Artemin appears to be the only member of the GDNF family that binds to and activates the GFRα3-receptor tyrosine kinase product of the c-ret proto-oncogene receptor complex[18] and is expressed in smooth muscle cells of the vessels during embryogenesis and has been considered to be a guidance factor encouraging sympathetic axonal projections.[19] Although the expression of artemin was found in a number of adult tissues, its function remains obscure, especially in skin.[18]

Here, we examine the involvement of endogenously expressed artemin from dermal fibroblasts in skin innervation and skin sensibility.

From [a]the Department of Dermatology, Course of Integrated Medicine, Graduate School of Medicine, Osaka University; [b]the Department of Dermatology, Cairo University; and [c]the Department of Dermatology, Kochi University.

This study was supported by the Ministry of Education, Culture, Sports, Science and Technology, Japan.

Disclosure of potential conflict of interest: The authors declare that they have no relevant conflicts of interest.

Received for publication February 18, 2012; revised April 20, 2012; accepted for publication May 23, 2012.

Available online July 4, 2012.

Corresponding author: Hiroyuki Murota, MD, PhD, Department of Dermatology, Course of Integrated Medicine, Graduate School of Medicine, Osaka University, 2-2, Yamadaoka, Suita-Shi, Osaka, Japan 565-0871. E-mail: h-murota@derma.med.osaka-u.ac.jp.

0091-6749/$36.00

http://dx.doi.org/10.1016/j.jaci.2012.05.027

Abbreviations used
AD: Atopic dermatitis
CM/SP: Conditioned medium derived from SP-treated NHDF
GDNF: Glial cell line–derived neurotrophic factor
GFRα: GDNF family receptor α
GFRα3 KO: GFRα3 knockout
NGF: Nerve growth factor
NHDF: Normal human dermal fibroblast
PDF: Primary dermal fibroblast
rARTN: Recombinant artemin
SP: Substance P
TRPV1: Transient receptor potential vanilloid 1

METHODS

Cell culture

A cultured normal human dermal fibroblast (NHDF) and SH-SY5Y, a neuroblastoma cell line, were purchased from Health Science Research Resources Bank (Osaka, Japan). Primary dermal fibroblasts (PDFs) were isolated from human adult skin samples. NHDF, PDFs, and HaCaT cells were cultured in Dulbecco modified Eagle medium (Gibco-BRL, Gaithersburg, Md) containing 10% fetal bovine serum (BioWhittaker, Inc, Walkersville, Md) and streptomycin at 37°C in a 5% CO_2 atmosphere. Murine embryonic fibroblastswere isolated and cultured as previously described.[20] SH-SY5Y was cultured in a 1:1 mixture of Essential Eagle's medium and Ham's F12 medium (both from Gibco-BRL) containing 10% fetal bovine serum. Normal human epidermal keratinocytes purchased from DS Pharma Biomedical (Osaka, Japan) were cultured in human keratinocyte serum-free medium (DS Pharma Biomedical).

Mice

Ten-week-old female mice were used in all experiments. C57BL/6 mice were purchased from Japan Clea (Osaka, Japan). GFRα3 knockout (GFRα3 KO) mice were described previously[21] and were a kind gift from Developmental Genetics Group, Graduate School of Frontier Biosciences, Osaka University. Mice were maintained in our pathogen-free animal facility. All animal care was in accordance with the institutional guidelines of Osaka University.

Slide culture of neuroblastoma cell line

SH-SY5Y cells were seeded in Lab-Tek chamber slides (NALGENE Labware, Rochester, NY). After 1 day in culture, cells were cultured with 50 ng/mL recombinant artemin (rARTN; R&D Systems, Minneapolis, Minn) or conditioned medium derived from 1×10^{-6} or 1×10^{-12} mol/L SP-treated NHDF after 12 hours of incubation. Three days after the addition of these factors, cells were photographed with a BZ-8000 microscope (Keyence, Osaka, Japan).

Cell proliferation assay

The proliferation rate was determined by using the cell proliferation ELISA BrdU assay kit (Cell Proliferation ELISA, BrdU, Roche, Mannheim, Germany). SH-SY5Ycells were cultured in the rARTN and SP-treated NHDF-derived conditioned medium with or without antiartemin antibody (R&D Systems), anti-GDNF antibody (Abcam, Cambridge, United Kingdom; ab10835), and anti–nerve growth factor (NGF)-β antibody (Chemicon, Temecula, Calif; AB1528) in a 96-well microplate at 37°C for 24 hours. Subsequently, BrdU incorporation was measured according to the manufacturer's instruction.

Histologic analysis

Samples of human and murine skin were cut on a cryostat to 20-μm thick sections.

For human healthy control skin and atopic dermatitis (AD), nummular eczema, prurigo nodularis, and psoriasis skin lesion biopsies, the antibodies used were goat antiartemin (sc-9331, Santa Cruz Biotechnology, Santa Cruz, Calif), rabbit antiartemin, goat anti-GFRα3 (both from R&D Systems), PGP-9.5 (Chemicon; AB1761), and vimentin (Dako, Carpentaria, Calif). Secondary antibodies were conjugated to Alexa Fluor 488 or 594 (Invitrogen, Carlsbad, Calif). For SP staining, 4-μm paraffin sections were incubated with primary antibodies (Abcam) and stained with the streptavidin-biotin amplification EnVision system (Dako).

For murine samples, the hindpaws of C57BL6 mice or GFRα3KO mice were intradermally injected once with 20 μL of 1×10^{-4} mol/L SP and 0.2 μg/20 μL recombinant mouse artemin (1085-AR/CF, R&D Systems). The dose setting of artemin injection was based on a previous report.[22] One day after administration, skin biopsy was performed at the injection site. The sections were incubated with primary antibody for SP (Abcam) and PGP9.5 (Chemicon) and visualized with fluorescein isothiocyanate or Alexa Fluor 594. Images were captured with a BZ-8000 microscope (Keyence).

Behavioral analysis

Response to infrared heat stimulus was measured with the tail flick test (Tail-flick unit; Ugo Basile, Comerio VA, Italy) and Hargreaves test (37370-Planter Test instrument, Ugo Basile). Mechanosensation was evaluated by Planter Test instrument (Ugo Basile). The effect of artemin and SP on thermal hyperalgesia was evaluated by using the Hargreaves test.[23] Animals were acclimated to the apparatus for 30 minutes before testing. The apparatus was set at a laser intensity of 60 (temperature after 10, 20, and 30 seconds was 42.0°C, 47.5°C, and 51.0°C, respectively), and testing was performed by using repeated measures (3-5 measures per foot) of the glabrous hindpaw skin. Three response times were averaged for each animal.

In experiments examining mouse behavior at warm temperatures, 0.2 μg/20 μL artemin or vehicle was given intradermally in interscapular on a Monday through Thursday schedule for a total of 4 injections over 2 weeks. One day after the final administration, mice were placed in constant warm temperature and a humid place (38°C and 60%, respectively). Mice were videotaped for 15 minutes following installation, and the time spent scratching or wiping was measured as described previously.[24] The transient receptor potential vanilloid 1 (TRPV1) antagonist, capsazepine (10 mg/kg), was administered intraperitoneally with a volume of 1 mL/kg before 5 minutes of investigation as described previously.[25]

RT-PCR

Total RNA was extracted with an RNeasy Mini kit (QIAGEN Gmbh, Hilden, Germany), according to the protocol provided by the manufacturer. First-strand cDNA was synthesized with an RT-PCR kit (Stratagene, La Jolla, Calif) by using oligo dT primers. The primers used for RT-PCR are presented in Table I. The ARTN primer set used for RT-PCR was purchased from SuperArray (Frederick, Md).

Real-time PCR

The levels of artemin, GDNF, and NGF mRNAs were analyzed by using Power SYBR Green PCR Master Mix (Applied Biosystems, Foster City, Calif) according to the manufacturer's protocols. Glyceraldehyde-3-phosphate was used to normalize mRNA levels. Sequence-specific primers are shown in Table I. The artemin primer set was purchased from SuperArray (Frederick, Md). Real-time PCR was performed on an ABI Prism 7000 sequence detector (Applied Biosystems).

Western blot analysis

NHDFs were washed with PBS twice, and approximately 5×10^5 cells were solubilized at 4°C in a lysis buffer. The protein extracts were analyzed with an antiartemin antibody (Santa Cruz). An antiactin antibody (Chemicon) was used as a control. For detection of Ser696-phosphorylated c-Ret,

TABLE I. Primer sequences for PCR

Gene	Accession no.	Sequences	
For RT-PCR			
NGF	NM_002506.2	Sense	5′-GAC AGT GTC AGC GTG TGG GTT-3′
		Antisense	5′-CCC AAC ACC ATC ACC TCC TT-3′
GDNF	NM_000514.3	Sense	5′-TTC GCG CTG AGC AGT GAC-3′
		Antisense	5′-TAC ATC CAC ACC TTT TAG CGG-3′
Neurturin	NM_004558.3	Sense	5′-CCT CAG TGC TCT GCA GCT C-3′
		Antisense	5′-TCG TGC ACC GTG TGG TAG-3′
GFRα1	NM_005264.4	Sense	5′-ACC AGC GTG TCC AAT GAT GT-3′
		Antisense	5′-AGG CAG TCA GCG TAG TTT TC-3′
GFRα2	NM_001495.4	Sense	5′-GCT GGC ATG ATT GGG TTT GA-3′
		Antisense	5′-TTG GAG TTG TTG GCC TTC AG-3′
GFRα3	NM_001496.3	Sense	5′-GTG TGA AAT GCT GGA AGG GT-3′
		Antisense	5′-TCA GGA GCA GAA TCA AGG GA-3′
GFRα4	NM_022139.3	Sense	5′-CTC TCC ATA CTT CCT GTC CT-3′
		Antisense	5′-CTA CAA AAG TGA CCC TCT CC-3′
GAPDH	NM_002046.3	Sense	5′-ACC ACA GTC CAT GCC ATC AC-3′
		Antisense	5′-TCC ACC ACC CTG TTG CTG TA-3′
For real-time PCR			
NGF	NM_002506.2	Sense	5′-CAG TTT TAC CAA GGG AGC AGC TT-3′
		Antisense	5′-CAA CAT GGA CAT TAC GCT ATG CA-3′
GDNF	NM_000514.3	Sense	5′-TTC GCG CTG AGC AGT GAC T-3′
		Antisense	5′-GCC ATT TGT TTA TCT GGT GAC CTT-3′

GAPDH, Glyceraldehyde-3-phosphate.

anti-phospho(Ser696) c-Ret antibody (Upstate, Charlottesville, Va) and anti-Ret antibody (Abcam) were used as primary antibodies.

Macroarray gene assay

Murine embryonic fibroblasts were prepared and cultured by using a previously described method.[21] At the subconfluent stage, cells were incubated with or without 1×10^{-6} mol/L SP or histamine (Sigma, St Louis, Mo) for 6 hours and total RNAs were isolated with an RNeasy kit (QIAGEN GmbH). The Panorama Mouse Cytokine Gene Array (Sigma) assay was performed according to the manufacturer's instructions. Gene expression signals were quantitated with a BAS5000 (Fujifilm, Tokyo, Japan).

In situ hybridization

Tissue sections were prepared and hybridized as described previously.[26] DIG-labeled riboprobes for artemin (human artemin transcript variant 2, accession: NM_057091, sequence position: 1452-1873) were prepared by using DIG RNA Labeling Mix (Roche, Indianapolis, Ind). A negative control riboprobe was purchased from Genostaff Co, Ltd (Tokyo, Japan). The sections were counterstained with Kernechtrot stain solution (Mutoh, Tokyo, Japan), dehydrated, and then mounted with Malinol (Mutoh).

Statistic analysis

Statistical significance was examined by unpaired *t* test or Bonferroni's multiple comparison test. Graph bars in the figures present mean ± SD.

Study approval

Human tissue samples were obtained with written informed consent, and the studies were approved by the institutional review board of Osaka University Hospital.

RESULTS

Artemin is induced in SP-treated dermal fibroblasts

The results in macroarray gene assays prompted us to focus on artemin, which is expressed in SP-treated fibroblasts, but not in mock- or histamine-treated murine embryonic fibroblasts (Fig 1, *A*). We then examined the expression of histamine and other members of the GDNF family in human dermal fibroblasts and keratinocytes by RT-PCR (Fig 1, *B*). Artemin expression was detected in normal human epidermal keratinocytes and spontaneously immortalized keratinocyte, HaCaT cells, but not in untreated PDFs or commercially available NHDF. GDNF expression was relatively high in NHDF and lower in PDFs and normal human epidermal keratinocytes. Neurturin mRNA was not detected in these cell types. To verify whether SP treatment influences the expression of artemin, GDNF, and NGF in NHDFs, mRNAs were examined by quantitative real-time PCR after treatment with various concentrations of SP (Fig 1, *C*). We found that the expression of artemin mRNA increased in an SP dose-dependent fashion. In contrast, the expression level of GDNF was not affected by SP treatment. The expression of NGF mRNA was upregulated, with peak expression at 1×10^{-12} mol/L SP (Fig 1, *C*). Western blotting analysis revealed that artemin protein could be detected 12 hours after SP treatment and became undetectable again after 24 hours (Fig 1, *D*).

Artemin accumulates in the dermis of AD skin lesions

To assess artemin expression levels in itchy skin diseases, skin sections derived from healthy controls and patients with AD were immunohistochemically stained to detect artemin (Fig 2, *A*). The epidermis and the dermis of AD skin lesions showed an intense staining pattern for artemin, whereas the pattern was weak in healthy control skin. Accumulation of artemin was also observed in nummular eczema lesional skin, and in prurigo nodularis and psoriasis, but with less intense staining (see Fig E1 in this article's Online Repository at www.jacionline.org). To determine the source of artemin, costaining with vimentin (Fig 2, *B*) and CD34 (Fig 2, *C*) was performed. Dermal fibroblasts (vimentin$^+$),

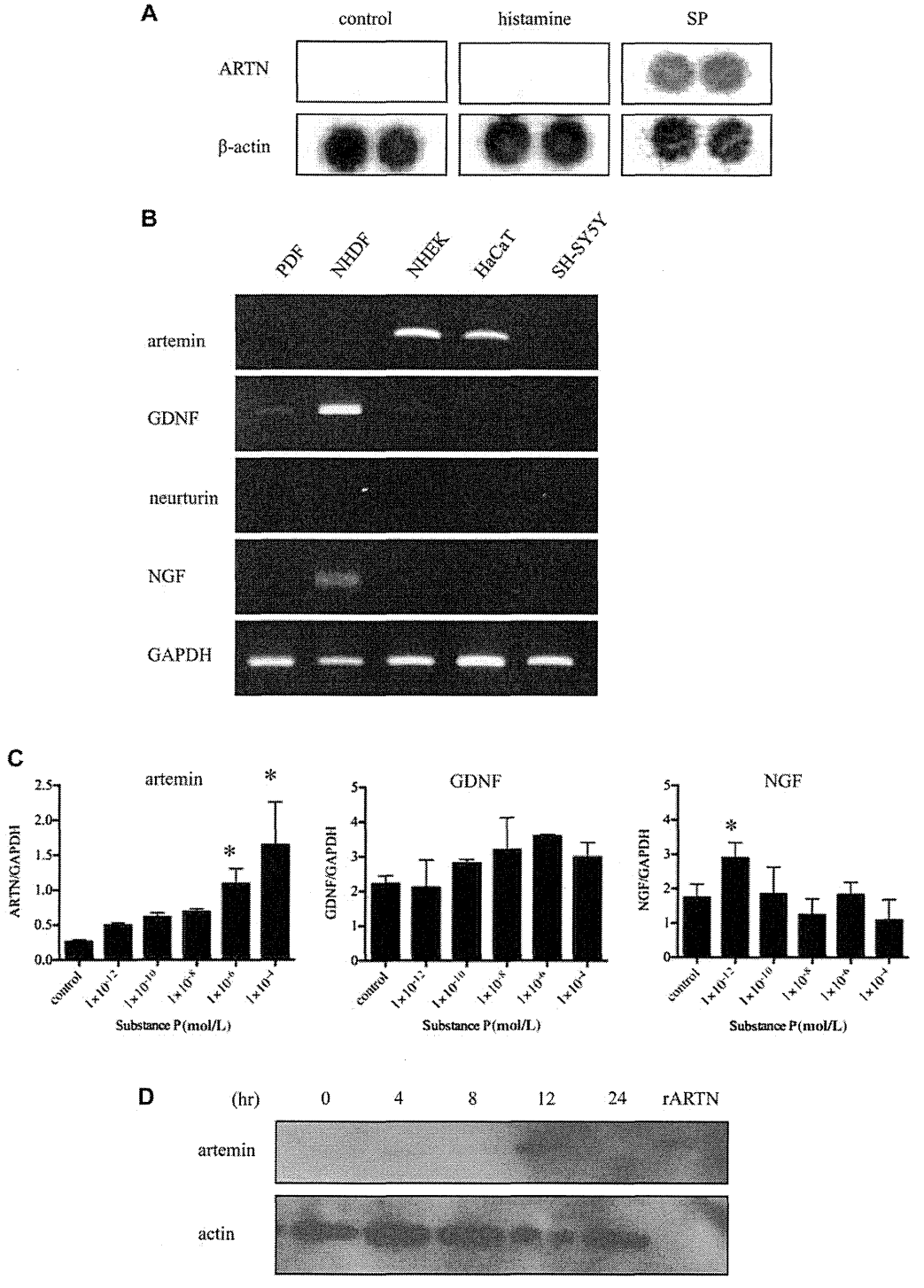

FIG 1. SP-treated fibroblasts express artemin. **A,** Result of macrogene array. Control: vehicle-treated. **B,** RT-PCR analysis of GDNF family, and NGF expression PDFs, NHDFs, and NHEKs. The data shown are representative of 2 independent experiments. **C,** Real-time PCR results in NHDF treated with various concentrations of SP for 6 hours. $*P < .05$. **D,** Sequential expression levels of artemin were examined by Western blot after treatment with 1×10^{-6} mol/L SP. *ARTN*, Artemin; *GAPDH*, glyceraldehyde-3-phosphate; *NHEKs*, normal human epidermal keratinocytes.

but not endothelial cells ($CD34^+$), in AD skin lesions costained for artemin. Although the number of dermal fibroblasts differed between healthy and diseased skin, the weak staining intensity of artemin in prurigo nodularis (also known as dermatitis with increased number of fibroblast[27]) indicates that the accumulation of artemin in the dermis of lesional skin is not simply a consequence of the altered number of dermal fibroblasts (see Figs E1 and E2 in this article's Online Repository at www.jacionline.org). *In situ*

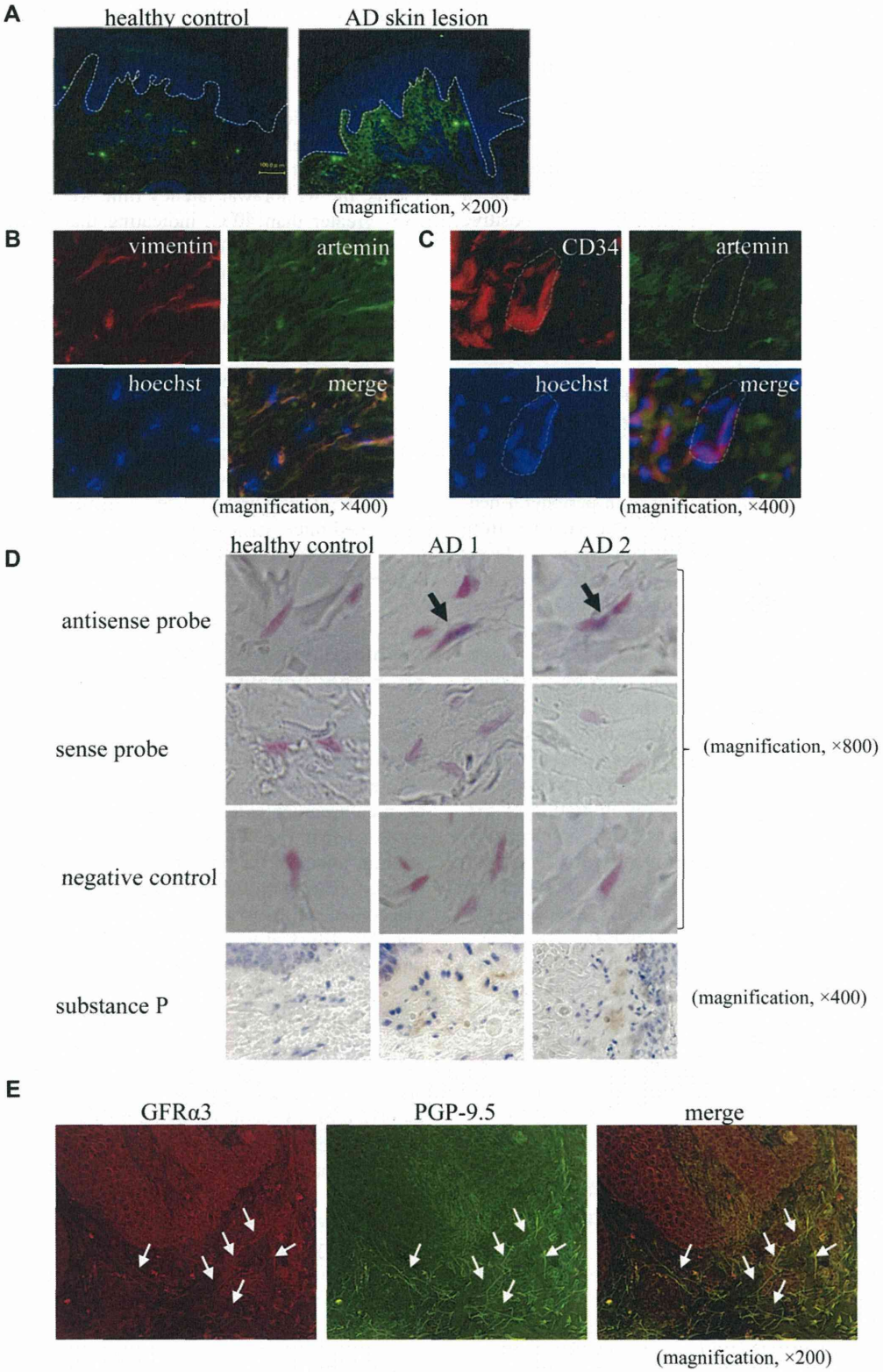

FIG 2. Accumulation of artemin in dermal fibroblasts from AD skin lesions. **A**, Healthy skin and an AD skin lesion (with disease duration of about 1 month) were stained for artemin. *Dashed white lines* represent the epidermal-dermal junction. AD skin lesion was costained for vimentin and artemin **(B)** or CD34 and artemin **(C)**. Hoechst: Hoechst 33342. *Dashed lines* represent the vascular wall (Fig 2, *C*). **D**, *In situ* hybridization for artemin. Positive signal appeared with blue (indicated by *arrows*). The disease duration was 4 days for AD1 and about 1 month for AD2. The same skin sections were immunostained for SP. **E**, Lesional skin with disease duration of about 1 month was immunolabeled with PGP-9.5 and GFRα3. *Arrows* indicate costained nerve fibers.

hybridization also revealed reproducible expression of artemin mRNA expression in the dermal fibroblasts of AD skin lesions but not in healthy skin (Fig 2, *D*). Increased numbers of SP-positive peripheral nerve fibers were also observed in the AD skin lesions (Fig 2, *D*, bottom).

Next, we were interested in determining whether artemin modulates the peripheral projection patterns of neurons. As expected, artemin-labeled, highly fluorescent dermal areas in AD skin lesions showed massive sprouting of PGP-9.5–positive peripheral neurons (see Fig E3 in this article's Online Repository at www.jacionline.org). Colabeling with anti-GFRα3 antibody proved that the sprouting nerve fibers in AD skin lesions were GFRα3-positive (Fig 2, *E*).

Artemin derived from SP-treated NHDFs induces strong differentiation and proliferation response in neuroblastoma cells

To compare the ability of the fibroblast-derived neurotrophic factors to influence a differentiation response in peripheral neurons, SH-SY5Y was cultured in conditioned medium derived from NHDF cultured with or without SP (Fig 3). The expression levels of GFRα1, GFRα2, and GFRα3 in SH-SY5Y cells suggest that this cell line responds to both GDNF and artemin (Fig 3, *A*). There was no significant difference in the morphology or proliferation of cells cultured with conditioned medium derived from mock-treated NHDF compared with those derived from fresh medium culture (Fig 3, *B* and *C*). An increase in the size of SH-SY5Y was observed with the conditioned medium derived from SP-treated NHDF (CM/SP) as well as rARTN treatment, but not in SH-SY5Y alone treated with SP (Fig 3, *B*). A BrdU incorporation assay revealed that CM/SP augmented the proliferation of SH-SY5Y (Fig 3, *C*). The role of artemin in CM/SP-induced SH-SY5Y proliferation was verified in experiments with an artemin neutralization antibody. Artemin neutralization inhibited the rARTN-induced proliferation of SH-SY5Y cells, whereas an isotype matched control antibody did not (see Fig E4 in this article's Online Repository at www.jacionline.org). As expected, artemin neutralization attenuated the CM/SP-induced proliferation of SH-SY5Y, whereas GDNF and NGF neutralization did not (Fig 3, *C*). Artemin neutralization also inhibited the phosphorylation of the receptor tyrosine kinase product of the c-ret proto-oncogene in SH-SY5Y cells cultured with rARTN or CM/SP (Fig 3, *D*).

Intradermal administration of artemin promotes peripheral nerve fiber sprouting and intraepidermal neurite outgrowth

The finding of high GFRα3 expression on sprouted peripheral nerve fibers led us to examine the possibility that artemin contributes to the peripheral nerve fiber sprouting. Wild-type mice were intradermally injected with artemin or SP 2 times per week for 2 weeks, and SP- or artemin-injected sites showed an increased number of peripheral nerve fibers, whereas nontreated (control) or vehicle-injected sites did not (Fig 4, *A*). Interestingly, artemin injection sites also displayed intraepidermal neurite outgrowth. As expected, the SP- or artemin-mediated nerve sprouting response was decreased in GFRα3KO mice (Fig 4, *B*), as was intraepidermal neurite outgrowth in artemin-injected sites (Fig 4, *B*).

Artemin is involved in thermal hyperalgesia

To explore whether artemin affects the cutaneous sensitivity to environmental stimuli, the intensity of perception was evaluated in GFRα3KO mice. The intensity of mechanosensation in GFRα3KO mice was comparable to that in wild-type mice (Fig 5, *A*). Next, thermal hyperalgesia was assessed by using Hargreaves test and a tail-flick test (Fig 5, *B* and *C*). In both experiments, the withdrawal latency time was prolonged at temperatures greater than 40°C, indicating that GFRα3KO mice have thermal hypoalgesia. To investigate the effect of artemin on thermal hyperalgesia, artemin-treated wild-type mice were examined for heat susceptibility by using Hargreaves test. As expected, a single administration of artemin induced thermal hyperalgesia (Fig 5, *D*).

SP has long been thought to elicit thermal hyperalgesia.[28] We also found that SP treatment shortened hindpaw withdrawal latency time after 12 hours (Fig 5, *E*). To confirm the involvement of artemin in SP-induced thermal hyperalgesia, artemin-neutralizing antibody was administered (Fig 5, *F*). Further prolongation of withdrawal latency time in artemin-neutralized, SP-treated mice was comparable to that in mice treated with SP alone, demonstrating a key role for artemin in SP-induced thermal hyperalgesia.

Administration of artemin to mice induced abnormal behavior in a warm environment

If artemin regulates thermal susceptibility, artemin-injected mice might display altered behavior when exposed to a warm environment. To verify this, mice received subcutaneous injection of artemin or vehicle into the interscapular region and were placed at an environmental temperature of 38°C, and their behavior was recorded with video imaging for 15 minutes. Surprisingly, artemin-injected mice showed wiping of the cheek (not the injection site) with forefoot starting about 3 minutes after being placed in a warm environment (see Video E1 in this article's Online Repository at www.jacionline.org). This abnormal behavior with stops at short intervals persisted to the end of the video recording and was confirmed by 2 repeated experiments (n = 3 for each experiment) (Fig 6, *A*). Vehicle-injected mice did not show any abnormal behavior in the 38°C environment. Both vehicle- or artemin-injected mice did not show behavioral differences at room temperature (data not shown). To confirm the involvement of GFRα3-mediated signaling in artemin-induced abnormal behavior, artemin-injected GFRα3KO mice were examined in the same behavioral assay. We found that artemin-injected GFRα3KO mice behaved like the vehicle-injected GFRα3KO mice and vehicle-injected wild-type mice (Fig 6, *B*) and did not display abnormal behavior. Capsazepine, a selective TRPV1-inhibitor, did not affect the artemin-induced abnormal behavior (Fig 6, *C*).

DISCUSSION

Artemin derived from SP-treated dermal fibroblasts was accumulated in AD-lesional skin and found to induce cutaneous nerve sprouting and cause rubbing behavior mimicking scratching warmth-evoked itch in mice.

In our study, artemin was strongly expressed on the dermis of skin biopsy slices from patients with AD. The homogenous staining pattern of artemin in the dermis is assumed to reflect the

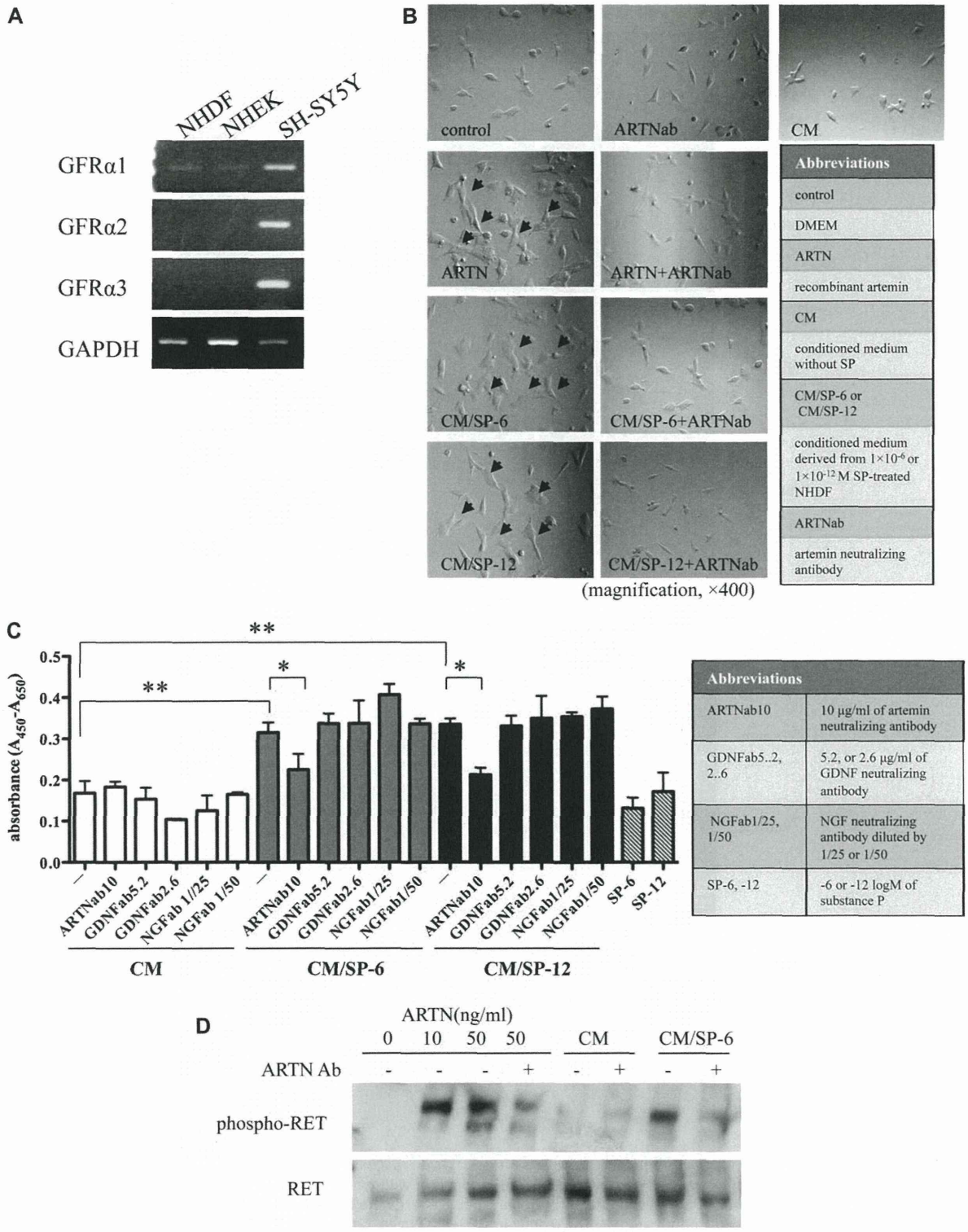

FIG 3. SH-SY5Y cells were cultured in conditioned medium derived from SP-treated NHDFs. **A,** RT-PCR analysis of the expression of GFRα family. **B,** Morphology of SH-SY5Y cells. Neurite outgrowth and neuronal morphology are indicated by *arrows*. **C,** The impact of artemin neutralization antibody on BrdU incorporation assay (n = 4). $*P < .05$, $**P < .01$. **D,** The impact of artemin neutralization antibody on the phosphorylation of RET in SH-SY5Y cells. *DMEM*, Dulbecco modified Eagle medium; *GAPDH*, glyceraldehyde-3-phosphate; *NHEK*, normal human epidermal keratinocyte; *Phospho-RET*, phosphorylated RET; *RET*, the receptor tyrosine kinase product of the c-ret proto-oncogene.

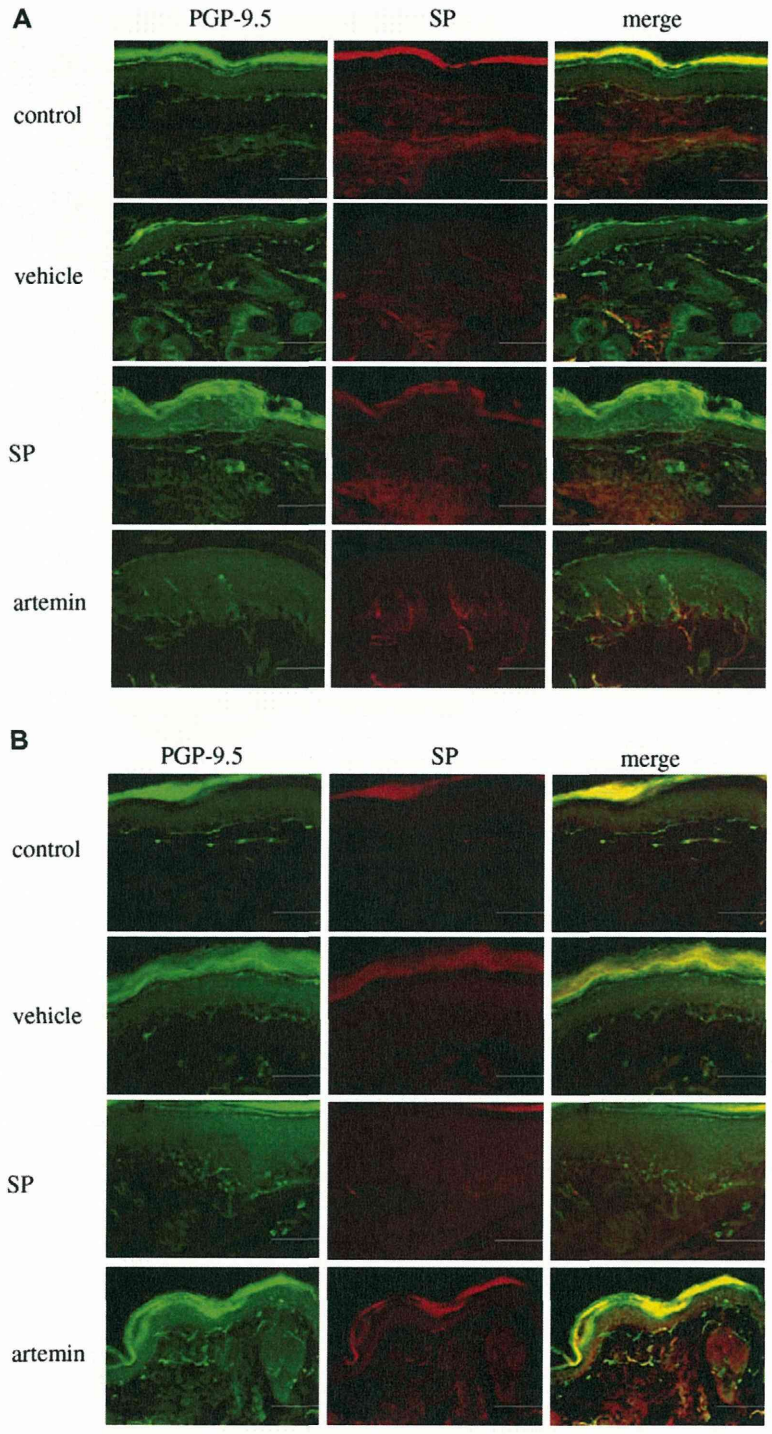

FIG 4. The effect of artemin on skin innervation. **A,** Hindpaws of wild-type mice were intradermally injected with vehicle, artemin, or SP, and cutaneous peripheral nerve fibers were stained with PGP9.5 *(green)* and SP *(red)*. Control indicates nontreated. **B,** The results in GFRα3KO mice. *Scale bar:* 100 μm.

heparin sulfate binding affinity of artemin.[29] The pathogenic influence of SP on dermal fibroblasts in many types of dermatoses, including scar tissue generated during wound healing,[30] stress-induced skin inflammatory responses,[31] and dermal fibrosing diseases, has been discussed.[32] There remains considerable debate, however, regarding the pathological involvement of dermal fibroblasts in forms of allergic dermatitis such as AD. Our findings support a novel role for dermal fibroblasts in which they may contribute to the neurobiological effects of SP in the pathogenesis of itchy allergic dermatitis.

In addition to SP-treated dermal fibroblasts, nontreated keratinocytes expressed artemin mRNA *in vitro* as well. However, artemin protein in nontreated keratinocytes was not detected *in vitro* (data not shown). It is not known how artemin protein expression is regulated, and this finding suggests that artemin gene expression in keratinocytes might be controlled at the posttranscriptional level.

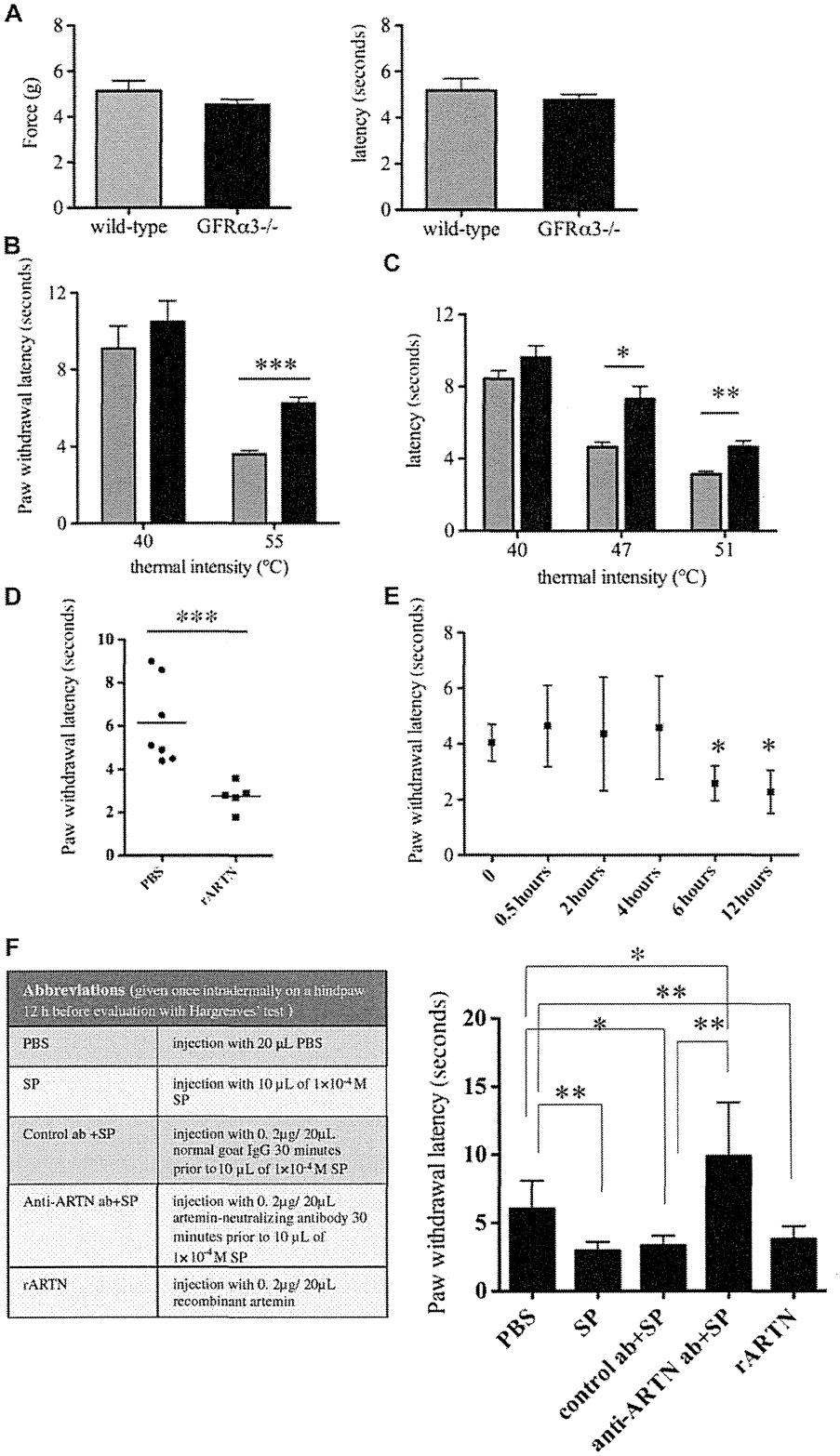

FIG 5. Dysesthesia in GFRα3KO mice. **A,** Mechanosensation of wild-type (n = 5) and GFRα3KO (n = 5) mice. Force and latency indicated the actual force and latency time at the time of paw withdrawal reflex, respectively. Response to infrared heat stimulus (latency and thermal intensity to paw withdrawal) was measured with **(B)** Hargreaves test and **(C)** tail-flick test. Gray and black bars show results for wild-type (n = 5) and GFRα3KO mice (n = 5), respectively. **D,** The effect of exogenously administered artemin on Hargreaves test (n = 5). **E,** The effect of exogenously administered SP on Hargreaves test results was evaluated over time (n = 5, $*P < .05$ [0.5 vs 4 hours]). **F,** The effect of artemin-neutralization antibody on SP-induced thermal hyperalgesia. $*P < .05$, $**P < .01$, $***P < .001$.

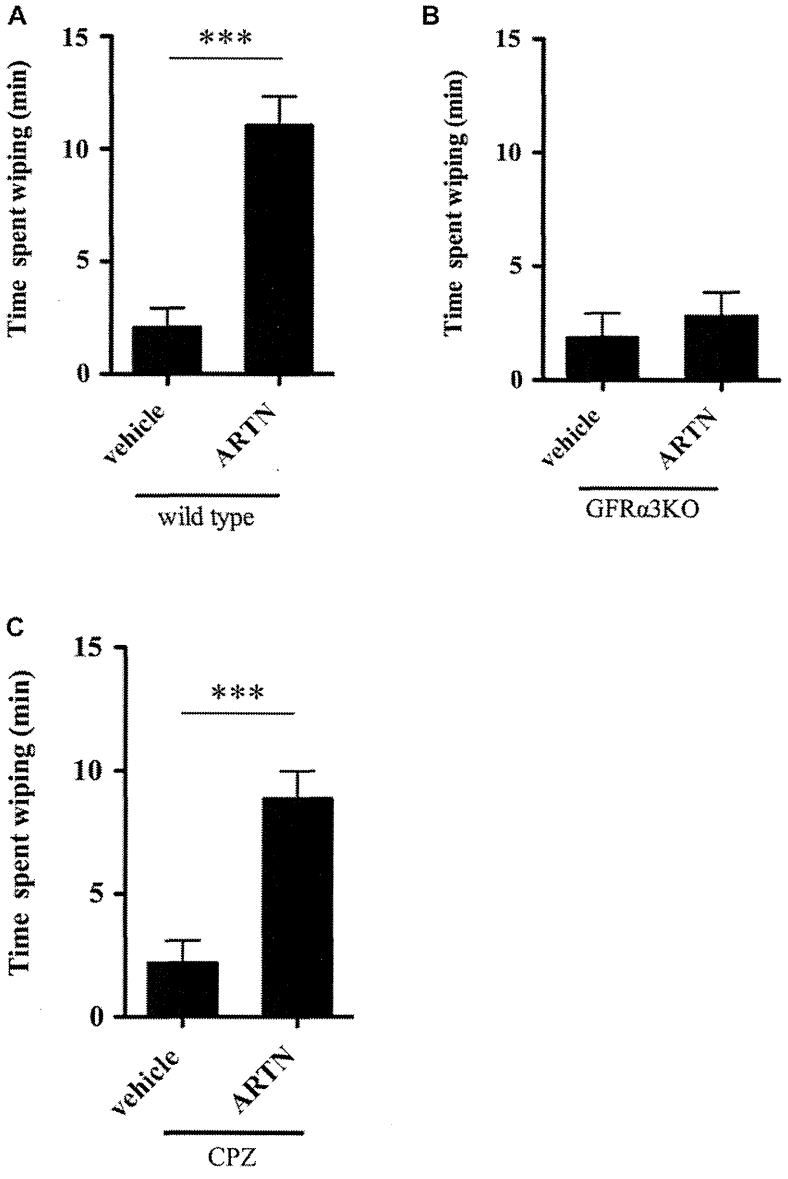

FIG 6. Artemin-injected mice showed abnormal behavior in warm conditions. **A,** Artemin-injected wild-type mice were videotaped, and the time spent wiping their cheek was measured. Representative of 2 independent studies (n = 3 in each experiment). **B,** Artemin-injected GFRα3KO mice were videotaped, and the time spent wiping their cheek was measured. Representative of 2 independent studies (n = 3 in each experiment). **C,** The impact of capsazepine (CPZ) on artemin-induced abnormal behavior was measured (n = 3). ***$P < .001$.

NGF, which is known to have an important effect on cells of both the nervous and immune systems,[33,34] is expressed at higher levels in chronic inflammatory disorders including AD.[35,36] Although the sources of NGF are mainly keratinocytes, mast cells, and skin cells, dermal fibroblasts also produce low levels of NGF under basal conditions, and NGF itself or TGF-β can enhance its production.[37] It has been reported that NGF and artemin play distinct and essential roles in the development of sympathic axons toward their final configurations.[18] Sympathetic neuron development requires signaling by chemoattractant artemin for migration and initial axon outgrowth. Once the nerve fibers reach their proper target, their survival and maintenance depend on target-derived NGF instead of artemin.[18] These findings suggest that coordinated expression of artemin and NGF is probably important in the sprouting and abnormal elongation of cutaneous nerve fibers, which is frequently observed in itchy allergic dermatitis. In this study, the expression of NGF and artemin mRNAs was differently regulated by the concentration of SP, indicating that the tissue concentration of SP might determine whether NGF or artemin plays a dominant role in disorganized skin innervation.

Dermal fibroblasts also expressed both GDNF and GFRα1, suggesting that autocrine secretion of neutrophic factors may regulate the homeostasis of skin including tissue remodeling and innervation. However, the neutralization of GDNF did not affect the proliferative activity of SH-SY5Y cells cultured with conditioned medium derived from SP-treated fibroblasts. At present, we have no data that address this conflicting finding regarding the function of GDNF.

Recently, Davis and coworkers[38] reported a phenotype of thermal hyperalgesia in transgenic mice that overexpress artemin in skin keratinocytes (K14-artemin Tg mice) and proposed that the phenotype is probably due to the upregulation of TRPV1 on cutaneous peripheral nerve fiber. As the complaint of intractable heat-provoked itch is frequently observed in patients with AD,[4] it may be that both artemin and TRPV1 are involved in this type of itch. Our findings confirm that artemin-treated mice show curious behavior similar to heat-provoked scratching. As the inhibition of TRPV1 with capsazepine administration did not affect the artemin-induced abnormal behavior, this phenotype is probably independent of TRPV1. Meanwhile, it was an unexpected outcome that artemin-injected mice rubbed their cheek in a warm environment but not the injection site. At present, we cannot explain the mechanism with concrete data, and take it as given that artemin might induce alloknesis throughout the whole body. Another interesting phenotype of K14-artemin Tg mice is the elongation of peripheral nerve fibers into the epidermis, which suggests a possible role for artemin in axon guidance.[38] In this study, we obtained data supporting this role for artemin, by confirming an effect of artemin on the elongation of the peripheral nerve fibers. We conclude that artemin has a considerable impact on both thermal susceptibility and innervation of skin.

As noted above, both prurigo nodularis accompanied by itch and psoriasis unaccompanied by itch displayed less intense staining for artemin than AD. Reduced intraepidermal nerve fiber density has been thought to be an indicator of subclinical cutaneous neuropathy,[39] which consistent with the reduced expression of artemin, an inducer of intraepidermal neurite outgrowth, was low in prurigo nodularis. Thus, the different results with the different types of lesions associated with itch indicate that altered artemin expression does not underlie itch in all skin disorders. Exploring the role of artemin in nummular eczema is a subject of future investigation. Our findings indicate that artemin may contribute to a novel mechanism for warmth-induced itch and that further investigation will yield a better understanding of the pathogenic involvement of SP in AD.

We thank Professor H. Hamada, Professor H. Shiratori, and Dr J. Nishino, Developmental Genetics Group, Graduate School of Frontier Biosciences, for providing GFRα3KO mice; Ms Ryoko Sugiyama and Ms Maiko Sugiura for secretarial work; and Mr Kenju Nishida, Mrs Yoshiko Nobuyoshi, Ms Sayaka Matsumura, and Mr Fu Han for research assistance.

Key messages

- Although warmth-evoked itch is a problem to be solved in AD, the underlying mechanism remains obscure.
- Artemin was induced by SP from dermal fibroblasts and accumulated in the dermis of AD-lesional skin.
- Artemin causes skin nerve fiber sprouting and thermohyperesthesia and developed warmth-evoked scratching behavior.

REFERENCES

1. Murota H, Kitaba S, Tani M, Wataya-Kaneda M, Azukizawa H, Tanemura A, et al. Impact of sedative and non-sedative antihistamines on the impaired productivity and quality of life in patients with pruritic skin diseases. Allergol Int 2010;59:345-54.
2. Koblenzer CS. Itching and the atopic skin. J Allergy Clin Immunol 1999;104:S109-13.
3. Bender BG, Leung SB, Leung DY. Actigraphy assessment of sleep disturbance in patients with atopic dermatitis: an objective life quality measure. J Allergy Clin Immunol 2003;111:598-602.
4. Wahlgren CF. Itch and atopic dermatitis: clinical and experimental studies. Acta Derm Venereol Suppl (Stockh) 1991;165:1-53.
5. Elias PM, Hatano Y, Williams ML. Basis for the barrier abnormality in atopic dermatitis: outside-inside-outside pathogenic mechanisms. J Allergy Clin Immunol 2008;121:1337-43.
6. Beltrani VS. The clinical spectrum of atopic dermatitis. J Allergy Clin Immunol 1999;104:S87-98.
7. Schmelz M. Itch–mediators and mechanisms. J Dermatol Sci 2002;28:91-6.
8. Ikoma A, Steinhoff M, Stander S, Yosipovitch G, Schmelz M. The neurobiology of itch. Nat Rev Neurosci 2006;7:535-47.
9. Heyer G, Ulmer FJ, Schmitz J, Handwerker HO. Histamine-induced itch and alloknesis (itchy skin) in atopic eczema patients and controls. Acta Derm Venereol 1995;75:348-52.
10. Hosogi M, Schmelz M, Miyachi Y, Ikoma A. Bradykinin is a potent pruritogen in atopic dermatitis: a switch from pain to itch. Pain 2006;126:16-23.
11. Hong J, Buddenkotte J, Berger TG, Steinhoff M. Management of itch in atopic dermatitis. Semin Cutan Med Surg 2011;30:71-86.
12. Baloh RH, Tansey MG, Lampe PA, Fahrner TJ, Enomoto H, Simburger KS, et al. Artemin, a novel member of the GDNF ligand family, supports peripheral and central neurons and signals through the GFRalpha3-RET receptor complex. Neuron 1998;21:1291-302.
13. Lin LF, Doherty DH, Lile JD, Bektesh S, Collins F. GDNF: a glial cell line-derived neurotrophic factor for midbrain dopaminergic neurons. Science 1993;260:1130-2.
14. Kotzbauer PT, Lampe PA, Heuckeroth RO, Golden JP, Creedon DJ, Johnson EM Jr, et al. Neurturin, a relative of glial-cell-line-derived neurotrophic factor. Nature 1996;384:467-70.
15. Milbrandt J, de Sauvage FJ, Fahrner TJ, Baloh RH, Leitner ML, Tansey MG, et al. Persephin, a novel neurotrophic factor related to GDNF and neurturin. Neuron 1998;20:245-53.
16. Durbec P, Marcos-Gutierrez CV, Kilkenny C, Grigoriou M, Wartiowaara K, Suvanto P, et al. GDNF signalling through the Ret receptor tyrosine kinase. Nature 1996;381:789-93.
17. Trupp M, Belluardo N, Funakoshi H, Ibanez CF. Complementary and overlapping expression of glial cell line-derived neurotrophic factor (GDNF), c-ret proto-oncogene, and GDNF receptor-alpha indicates multiple mechanisms of trophic actions in the adult rat CNS. J Neurosci 1997;17:3554-67.
18. Airaksinen MS, Saarma M. The GDNF family: signalling, biological functions and therapeutic value. Nat Rev Neurosci 2002;3:383-94.
19. Honma Y, Araki T, Gianino S, Bruce A, Heuckeroth R, Johnson E, et al. Artemin is a vascular-derived neurotropic factor for developing sympathetic neurons. Neuron 2002;35:267-82.
20. Murota H, Hamasaki Y, Nakashima T, Yamamoto K, Katayama I, Matsuyama T. Disruption of tumor necrosis factor receptor p55 impairs collagen turnover in experimentally induced sclerodermic skin fibroblasts. Arthritis Rheum 2003;48:1117-25.
21. Nishino J, Mochida K, Ohfuji Y, Shimazaki T, Meno C, Ohishi S, et al. GFR alpha3, a component of the artemin receptor, is required for migration and survival of the superior cervical ganglion. Neuron 1999;23:725-36.
22. Malin SA, Molliver DC, Koerber HR, Cornuet P, Frye R, Albers KM, et al. Glial cell line-derived neurotrophic factor family members sensitize nociceptors in vitro and produce thermal hyperalgesia in vivo. J Neurosci 2006;26:8588-99.
23. Hargreaves K, Dubner R, Brown F, Flores C, Joris J. A new and sensitive method for measuring thermal nociception in cutaneous hyperalgesia. Pain 1988;32:77-88.
24. Wilson SR, Gerhold KA, Bifolck-Fisher A, Liu Q, Patel KN, Dong X, et al. TRPA1 is required for histamine-independent, Mas-related G protein-coupled receptor-mediated itch. Nat Neurosci 2011;14:595-602.
25. Mallet C, Barriere DA, Ermund A, Jonsson BA, Eschalier A, Zygmunt PM, et al. TRPV1 in brain is involved in acetaminophen-induced antinociception. PLoS One 2010;5:pii:e12748.
26. Terao M, Murota H, Kitaba S, Katayama I. Tumor necrosis factor-alpha processing inhibitor-1 inhibits skin fibrosis in a bleomycin-induced murine model of scleroderma. Exp Dermatol 2010;19:38-43.
27. Weigelt N, Metze D, Stander S. Prurigo nodularis: systematic analysis of 58 histological criteria in 136 patients. J Cutan Pathol 2010;37:578-86.
28. Nemeroff CB, Osbahr AJ III, Manberg PJ, Ervin GN, Prange AJ Jr. Alterations in nociception and body temperature after intracisternal administration of neurotensin, beta-endorphin, other endogenous peptides, and morphine. Proc Natl Acad Sci U S A 1979;76:5368-71.

29. Silvian L, Jin P, Carmillo P, Boriack-Sjodin PA, Pelletier C, Rushe M, et al. Artemin crystal structure reveals insights into heparan sulfate binding. Biochemistry 2006;45:6801-12.
30. Lai XN, Wang ZG, Zhu JM, Wang LL. Effect of substance P on gene expression of transforming growth factor beta-1 and its receptors in rat's fibroblasts. Chin J Traumatol 2003;6:350-4.
31. Bae SJ, Matsunaga Y, Takenaka M, Tanaka Y, Hamazaki Y, Shimizu K, et al. Substance P induced preprotachykinin-a mRNA, neutral endopeptidase mRNA and substance P in cultured normal fibroblasts. Int Arch Allergy Immunol 2002;127:316-21.
32. Katayama I, Nishioka K. Substance P augments fibrogenic cytokine-induced fibroblast proliferation: possible involvement of neuropeptide in tissue fibrosis. J Dermatol Sci 1997;15:201-6.
33. Lambiase A, Bracci-Laudiero L, Bonini S, Starace G, D'Elios MM, De Carli M, et al. Human CD4+ T cell clones produce and release nerve growth factor and express high-affinity nerve growth factor receptors. J Allergy Clin Immunol 1997;100:408-14.
34. Sin AZ, Roche EM, Togias A, Lichtenstein LM, Schroeder JT. Nerve growth factor or IL-3 induces more IL-13 production from basophils of allergic subjects than from basophils of nonallergic subjects. J Allergy Clin Immunol 2001;108:387-93.
35. Bonini S, Lambiase A, Angelucci F, Magrini L, Manni L, Aloe L. Circulating nerve growth factor levels are increased in humans with allergic diseases and asthma. Proc Natl Acad Sci U S A 1996;93:10955-60.
36. Dou YC, Hagstromer L, Emtestam L, Johansson O. Increased nerve growth factor and its receptors in atopic dermatitis: an immunohistochemical study. Arch Dermatol Res 2006;298:31-7.
37. Micera A, Vigneti E, Pickholtz D, Reich R, Pappo O, Bonini S, et al. Nerve growth factor displays stimulatory effects on human skin and lung fibroblasts, demonstrating a direct role for this factor in tissue repair. Proc Natl Acad Sci U S A 2001;98:6162-7.
38. Elitt CM, McIlwrath SL, Lawson JJ, Malin SA, Molliver DC, Cornuet PK, et al. Artemin overexpression in skin enhances expression of TRPV1 and TRPA1 in cutaneous sensory neurons and leads to behavioral sensitivity to heat and cold. J Neurosci 2006;26:8578-87.
39. Schuhknecht B, Marziniak M, Wissel A, Phan NQ, Pappai D, Dangelmaier J, et al. Reduced intraepidermal nerve fibre density in lesional and nonlesional prurigo nodularis skin as a potential sign of subclinical cutaneous neuropathy. Br J Dermatol 2011;165:85-91.

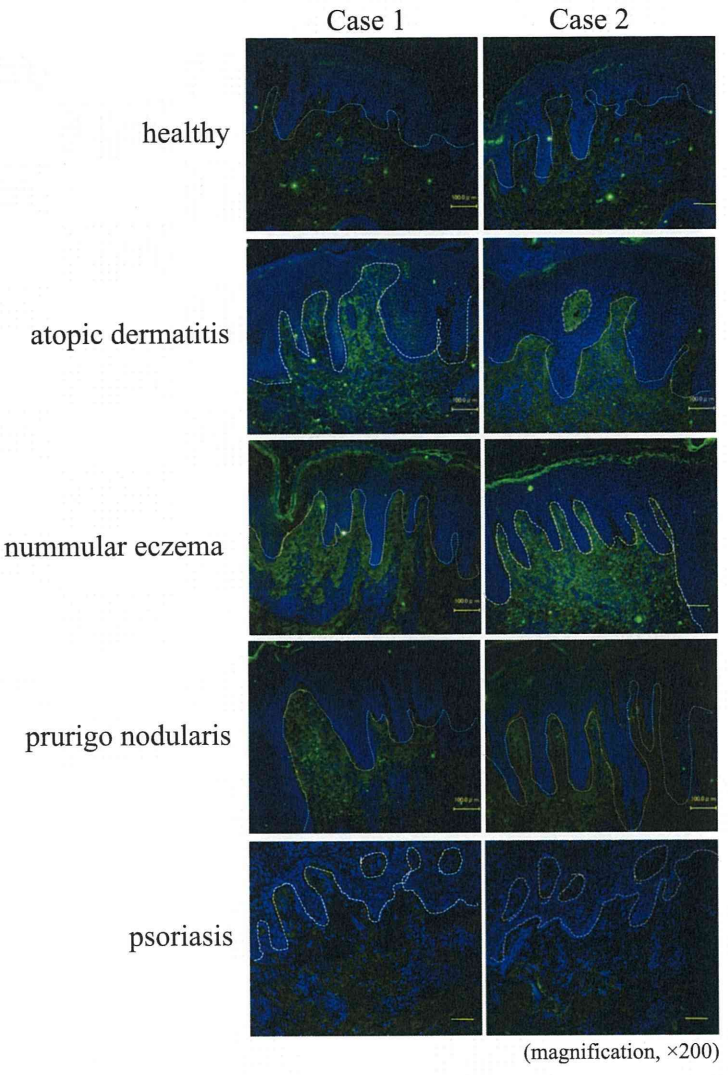

FIG E1. Immunohistochemical staining for artemin *(green)* was performed with healthy skin and 2 AD skin lesions (disease duration of case 1 and case 2 was about 1 week and 3 months, respectively), nummular eczema skin lesions (disease duration of case 1 and case 2 was about 1 month and 2 months, respectively), prurigo nodularis skin lesions (disease duration of case 1 and case 2 was about 1 year and about 6 months, respectively), and psoriasis skin lesions (disease duration of case 1 and case 2 was about 1 week and about 1 month, respectively). *Blue*: Hoechst 33342. *Dashed white lines* represent the epidermal-dermal junction. *Scale bar:* 100 μm.

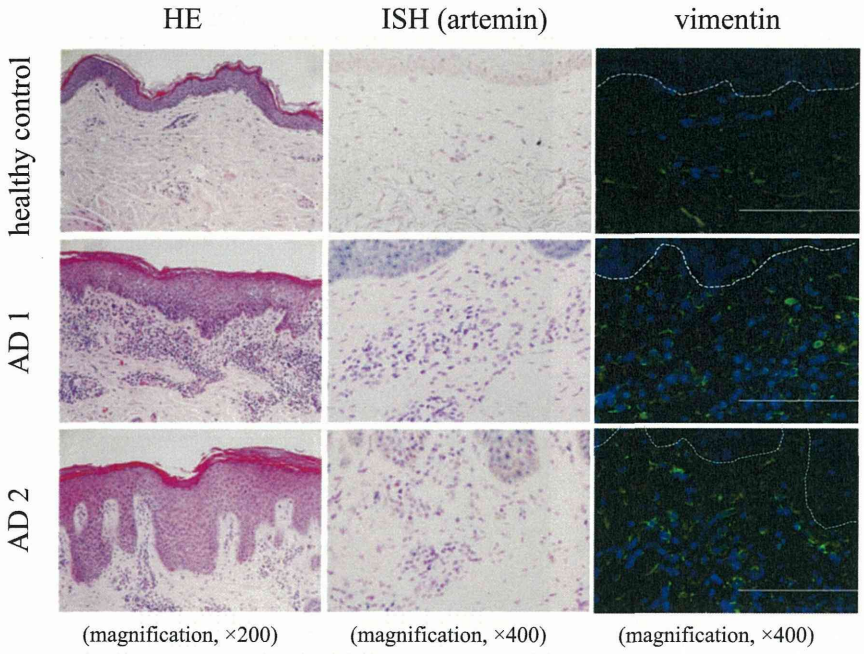

FIG E2. To compare the number of dermal fibroblasts, healthy skin and 2 AD skin lesions (AD1 and AD2), which were identical to the sample in ISH analysis (Fig 2, *D*), were costained for vimentin. Results of hematoxylin and eosin *(HE)* staining and ISH for artemin (*purple* indicates a positive signal) are shown alongside vimentin-stained images (*green*: vimentin, *blue*: Hoechst 33342). *Dashed white lines* in the vimentin-stained images represent the epidermal-dermal junction. *ISH, In situ* hybridization.

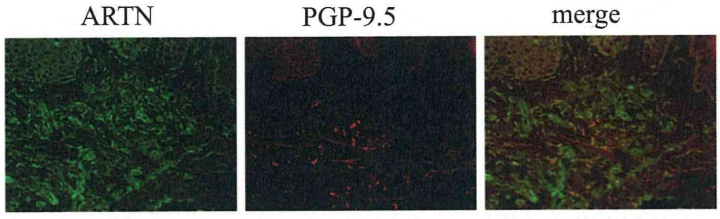

FIG E3. Skin innervation in AD lesional skin was examined by immunolabeling for PGP-9.5 and artemin. PGP-9.5–positive peripheral nerve fibers *(red)* showed massive sprouting in the area with artemin accumulation *(green)* (magnification ×400).